Using Maxwell's Z-Model to Determine Lunar Mare Lava Thickness

A Senior Honors Thesis
Bemidji State University

Autumn Wille

Research Guided by
Jason Dahl

Abstract

This project uses existing mathematical models of impact ejecta motion during crater formation to relate original material depth within a target to its final ejected distance from the crater. The resulting model equations were then used to estimate the maximum thickness of mare basalts at the locations of several lunar craters, and the results were compared Thomson's current work in the examination of lunar mare thickness.
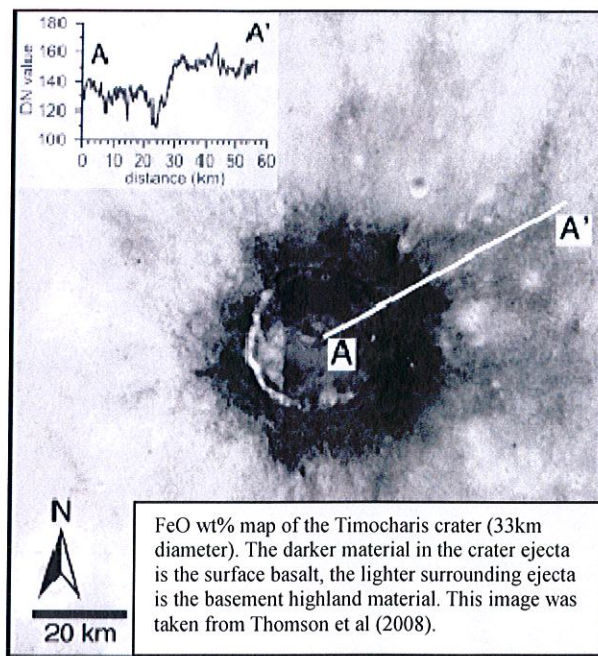
Introduction

Remote sensing of impact craters may be one of the most effective ways to study planetary surface histories through depositional and erosional features. We can use this information to determine surface age, thermal evolution and surface rock origins. It is also a prime way to determine sub-surface material composition as well as type and effect of impactors. When a projectile strikes a planetary surface the material of the impactor itself and the material near the surface are ejected in a very fast, high-energy process. Though some of the material is vaporized on impact, much of it is distributed around the crater with the deepest material lying closest to the crater itself and the shallower material coming to rest far out into the rays of the ejecta (Shoemaker, 1963). A potential application of impact crater ejecta studies is in examining material under the surface that we cannot currently excavate.

The iron-rich lunar maria cover much of the Moon's surface; they are volcanic in origin and overlie older lunar highland crust which contains much less iron. When a there is a small impact, ejecta contains only shallow mare material; when there is a larger impact, the ejecta will contain both iron-

rich mare basalt and also the deeper, low-iron basement rock. Material ejected on the surface will

represent the inverted order of the layers below (Shoemaker, 1963). The difference in iron content is

apparent under processing in the spectral imagery obtained by the Clementine spacecraft (See figure 1).

When a crater is deep enough to have a significant amount of basement material in the ejecta, it appears

like a halo around the crater at a roughly uniform radius. This radius can be used to determine the

original material depth.

Figure 1.

FeO wt% map of the Timocharis crater (33km diameter). The darker material in the crater ejecta is the surface basalt, the lighter surrounding ejecta is the basement highland material. This image was taken from Thomson et al (2008).

Thomson *et.al* (2008) is currently using crater ejecta data from the lunar surface to examine the

original thickness of the mare. His process estimates the basalt thickness using crater topographic and

spectral data obtained from the Clementine Mission. An analysis of the iron content in the ejecta

displays the radius of the basement material. The depth of the transient crater was inferred from known

ratios of crater geometry. Thomson assumes that the ratio of continuous ejecta to that of the basement

ejecta is linearly related to the corresponding material depths. From this assumption he developed a

geometric relation to find basalt depth.

History

The process that moves material during the formation of an impact crater is complex, but years of study have gone into the simplification of models that represent the motion with reasonable accuracy. Donald Maxwell (1977) developed a simple model for explosive cratering that has later been altered to work for impacts. The model describes the path that a particle follows from impact center along what is referred to as a streamline. The functions are based on the assumption that the flow is incompressible and that the trajectories of ejecta above the ground plain *plane?* are independent as a result of spall. Finally the model assumes that the radial component of velocity below the ground plain is derived from the strength flow coefficient over the polar radius to the power of Z. This Z in Maxwell's Z-model controls the shape or curve of the stationary stream lines below the surface.

In 1980, Steven Croft published a paper analyzing the Z model in terms of impact craters. His research included measurements of explosion craters where the charge was set at a depth below the surface, or at the EDOZ. He compiled information about ratios from radius to depth and he derived, from the Z model, a series of equations for most geologic features and geometric relations of a crater. He then applied these ratios to existing models of lunar maria depths and found that they were likely off by factors of two or three. He was also able to draw conclusions about the geometric similarities for craters of any size. From many of these assumptions, ratios can be drawn that are useful in later assumptions of this project.

The volumes of material ejected from lunar basins were examined by J.W. Head et al. in 1975.

He noted that the two ways to evaluate these volumes would be either to measure evidence of material around the crater and missing from within the crater basin, or to mathematically derive it with knowledge of small impact morphology. He noted that one third to one half of the apparent depth of a crater was actually created by compression in some materials, so the visual depth of a crater does not necessarily infer the depth of the material found in the ejecta. This is why finding depths through mathematical models (which assume incompressible flow) is essential for small impacts. Models are also more valid then using an assessment of surrounding ejecta for volumes because material in the ejecta may vaporize and may also contain impactor material.

Work done on flow-field center migration (Anderson et al., 2006) not only examined the theory that the depth of burst must be below the surface but actually tracked the movement of this depth as is related to time. Using NASA Ames Vertical Gun Range to simulate impacts, Anderson was able to observe the momentum transfer into the material and recognized that non-dimensional scaling for impacts only works when the impact angle is vertical. Anderson also noted that a consequence of applying Maxwell's model center at a depth below the surface results in having the earliest streamlines pointing back into the center of the crater making the angles higher than is represented in lab experimentation (Anderson et al. 2003).

Thomsen and Austin *et al.* did research using a small (0.3g) impactor into plasticene clay and examined the effects on Maxwell's model of a time dependent flow strength coefficient (alpha) and Z. Data for the lab experiments were recorded in early-time (through 18μsec) and also in later-time (18μsec to 600μsec) growth of the crater. Regressions were applied to account for the variability of alpha and Z dependent on different depths of the flow field center. This experiment was also expanded to using gabbroic anorthosite (similar to lunar composition) as the impact material. It was from these

works that our assumptions about alpha were derived (Thomsen et al. 1979, Austin et al. 1980, Austin et al. 1981).

Method

For this study, we use Maxwell's Z model, incorporating modifications by Croft, to derive estimates of maximum mare lava thickness at several locations. Several assumptions are required to develop mare thickness estimates. These assumptions and the equations used will be expanded on now.

Initial Assumptions

The first assumption for this project is that craters were formed from a near vertical impact. While it has been shown that most impacts happen at 45 degree angles or less from the surface (Shoemaker, 1962); a vertical impact model represents all but the lowest angle impacts with a reasonable degree of accuracy for the extent of this project (Anderson et al. 2006).

Using a lunar environment established many other assumptions for this project. This environment is ideal because of the simplicity of ejecta motion in a vacuum. A lunar environment is also highly relevant to the outcome of understanding material depth to ejecta distance relations because of the layer of Maria over much of the lunar surface. Assuming a lunar environment establishes gravity to be about 1.622 m/s^2 and for convenience, also establishes the units for the rest of this project to be in meters. It also establishes a lack of atmospheric drag.

Because the data for this project were derived from known relations rather than lab experimentation, several assumptions had to be made about the constants, ratios, and other aspects of the impact. Maxwell's Z-model, which is a point source model used for its simplicity and analytical development, demonstrates a correlation to existing data to a good degree for this project. Three of the most important parameters in this model are the Z which characterizes the streamline shape (figure 2), the strength flow coefficient alpha, and the effective depth of the Z-model (EDOZ). Austin and Thomsen, *et al.* worked with .3g projectiles in plasticene modelling clay and evaluated Maxwell's model for alpha and Z during the early formation of the crater. Their results found Maxwell's model reasonable assuming the Z-model center was below the surface by about one projectile diameter (Thomsen et al. 1979). This is confirmed by Croft (1980). They also continued the study into the later-time crater growth and examined the effect of a constant or variable Z and alpha. It was found that if alpha and Z are held fixed, the EDOZ must move downward to maintain agreement with their data. In other words, both alpha and Z displayed a time dependant variable relationship throughout crater growth (Austin et al. 1980).

Figure 2: Z and Streamline Shape.

$$Z = 2 \quad \theta_e = 0° \qquad Z = 3 \quad \theta_e = 45° \qquad Z = 4 \quad \theta_e = 63°$$
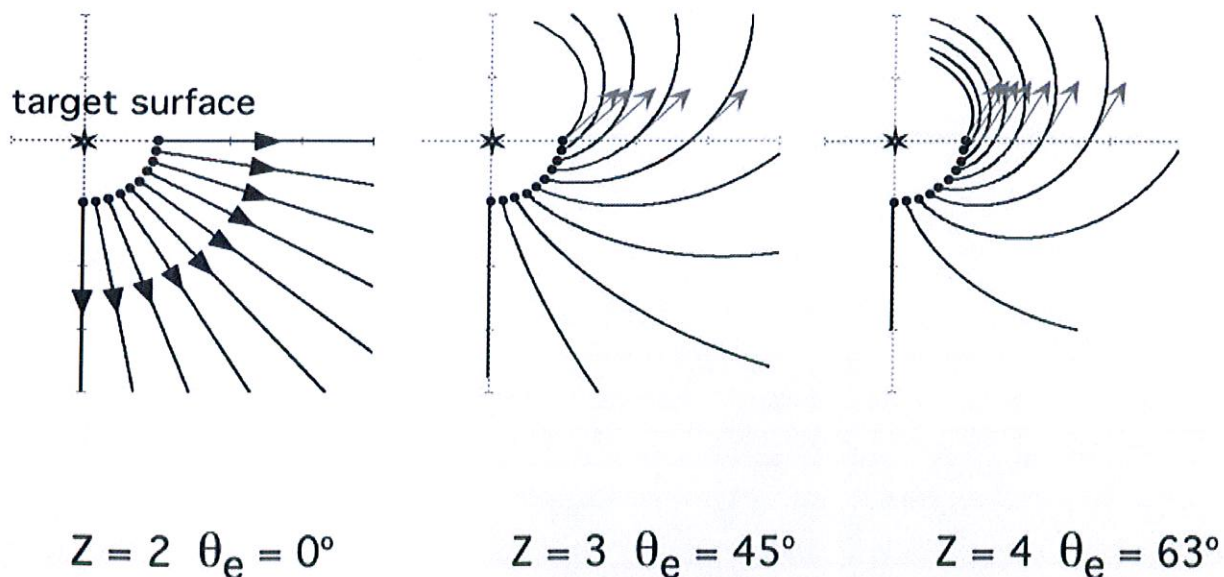
This figure was taken directly from Anderson *et al.* (2004) and uses Croft's (1980) modified streamline equation from Maxwell's Z model.

In the work done by Croft (1980) there is an agreement that a constant alpha, Z and EDOZ cannot accurately represent an impact. However he also found that the Z and EDOZ can remain constant with a variable alpha and still represent the streamlines to a good degree, especially during the latter half of the crater excavation, which is the portion of interest for this study. In this study, we chose to follow this idea and assumed a constant Z and EDOZ and developed an equation for a time-dependant alpha. The Z for this study was kept at 2.71 which was found reasonable in Maxwell's work and was used in other research including Croft (1980), Austin *et al.* (1981), and Anderson *et al.* (2003). We also used an EDOZ of about one projectile diameter (Austin et al 1980, Croft 1980).

The projectile diameter itself had to be derived from the final size of the crater; this was done assuming, as we can with many other aspects of crater geometry, that there is a relatively constant ratio in sizes. In this case data was used from Austin *et al.* (1981) in which a calculation was run for an iron projectile of 62.4 meters in diameter, projected into a gabbroic anorthosite material (which is similar to the lunar surface composition) leaving a 900 meter diameter crater. This ratio means the impactor radius is then roughly 0.138 the size of the final crater radius. This ratio was used for the EDOZ.

Mathematical Assumptions

Many of the following assumptions were derived from the appendix of Croft's work (1980) and will use the same notation (See fig. 3). A table was built through Microsoft Excel using these formulas to show the geometric relations as a function of the percent of the crater growth. All relations are

initially dependant on the final apparent radius size which can be entered into a single box in meters to

recalculate the contents of the table. Each column of the table is a different variable in the crater

geometry and the derivations for these variables will now be explained.

Fig 3. Geometry of a Streamline.
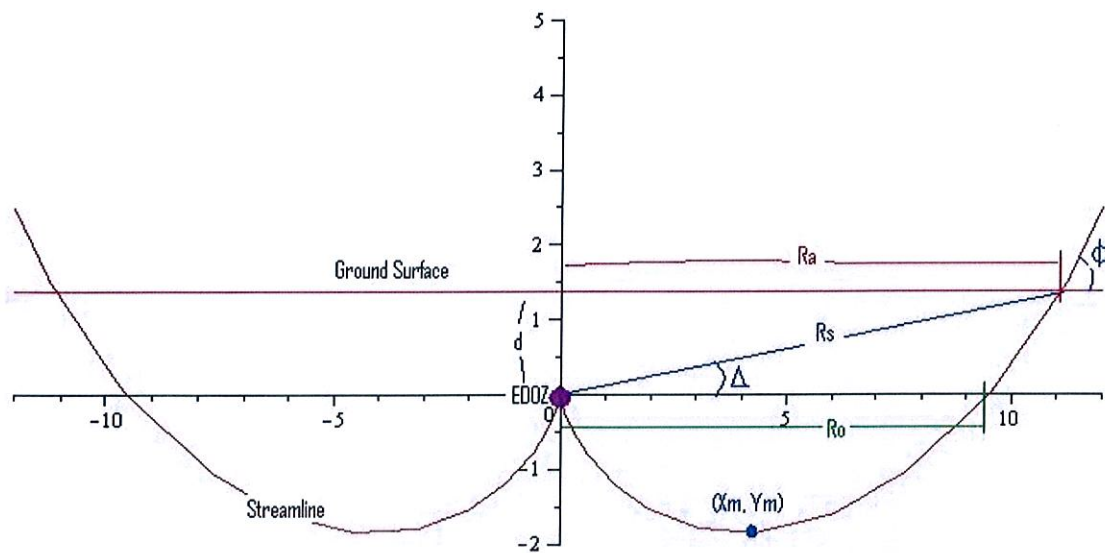
This diagram shows a streamline originating at the axis center at depth d from ground level. Ro is the radius of the crater parallel with the

EDOZ. Ra is the radius from the center of impact to the edge of the crater rim at the surface, and Rs is the radius from the EDOZ to the

surface crater rim. Δ is the angle from horizontal from the EDOZ to the ground surface at the final crater rim and φ is the angle of the

ejecta trajectory at the surface. The point (Xm, Ym) is the horizontal and vertical coordinates of the maximum depth of the streamline.

The apparent radius or Ra of a crater is the final visual radius at the surface. Throughout formation of the crater this radius is only a percentage of its final size and so this percentage was used as a marking point for various stages throughout crater growth. Below this surface level is the Z-model origin at the EDOZ noted previously which is at depth d. From this EDOZ to the far edge of the Ra is a length denoted as Rs which is the Z-model radius at the surface level. It was calculated by:

1) $Rs = \sqrt{(d^2 + Ra^2)}$

The angle from the horizontal from this EDOZ center to the edge of Ra along Rs is noted by Δ.

2) $\Delta = \arctan(d/Ra)$

A simplified streamline equation is given by Croft (1980)

3) $R = Ro(1 - \cos(\theta))^{\frac{1}{Z-2}}$

Knowing Rs, which is the radius of the streamline equation at the surface, it becomes possible to solve for Ro, which is the radius of the streamline equation parallel with the EDOZ.

4) $Ro = Rs/((1 + \sin(\Delta))^\wedge(1/(Z-2)))$

Ym is the maximum depth of the final crater and is given by Croft (1980) as:

5) $Ym = Ro(Z-2)[Z-1]^{\frac{1-Z}{Z-2}} + d.$

The final points of detail are relating to the trajectory and material in the ejecta above the ground surface. The first of these functions is the velocity and angle of ejection which is dependent on alpha and was taken from Maxwell (1977). The radial and angular components are:

6) $Ur = \alpha R^{-Z}$

7) $U\theta = \alpha R^{-Z} * (Z-2) * \sin\theta/(1 + \cos\theta)$

In these equations R is at the surface so Rs can be used. From these equations Ux and Uy can be derived, the derivations presented by Croft (1980) were used. Also taken from Croft's appendix was the ejection angle $\emptyset$:

8) $\emptyset = \tan^{-1} * \left[\dfrac{\frac{\tan\Delta}{\cos\Delta} - \tan^2\Delta + (Z-2)}{\frac{1}{\cos\Delta} - \tan\Delta\,(Z-1)}\right]$

The distance from the crater rim to the final location of the ejecta can be derived from trajectory equations knowing the gravity and horizontal velocity of this distance or Xg is:

9) $Xg = Vx * 2Vy/g + Ra$.

The Flow Strength Problem

When developing the relations for impact craters in lunar conditions, it was noted that a constant strength flow coefficient alpha gave unrealistic results, which was consistent with Croft's (1980) conclusions that Z, EDOZ, and alpha cannot all be kept constant. But having a time-dependent alpha requires a function to relate it to the crater formation. This was developed using the data collected by Austin *et al.* (1980) for a .3 g aluminum projectile in plasticene clay material during crater development from 18 μsec to 600 μsec.

Austin's published results for alpha at 90 degrees from EDOZ were plotted against time. Also published were the crater depths throughout growth during the same time frame. Using those depths and Croft's derivation for the maximum depth, (Croft 1980) the radius Ro was derived for those times. Having both alpha and crater radius as time dependant functions allowed the two functions to be plotted against each other, and the crater radius was converted into a percent of the final crater size to negate the units. When this data was plotted, Microsoft Excel was used to find a suitable power regression. This regression showed the flow strength to be:
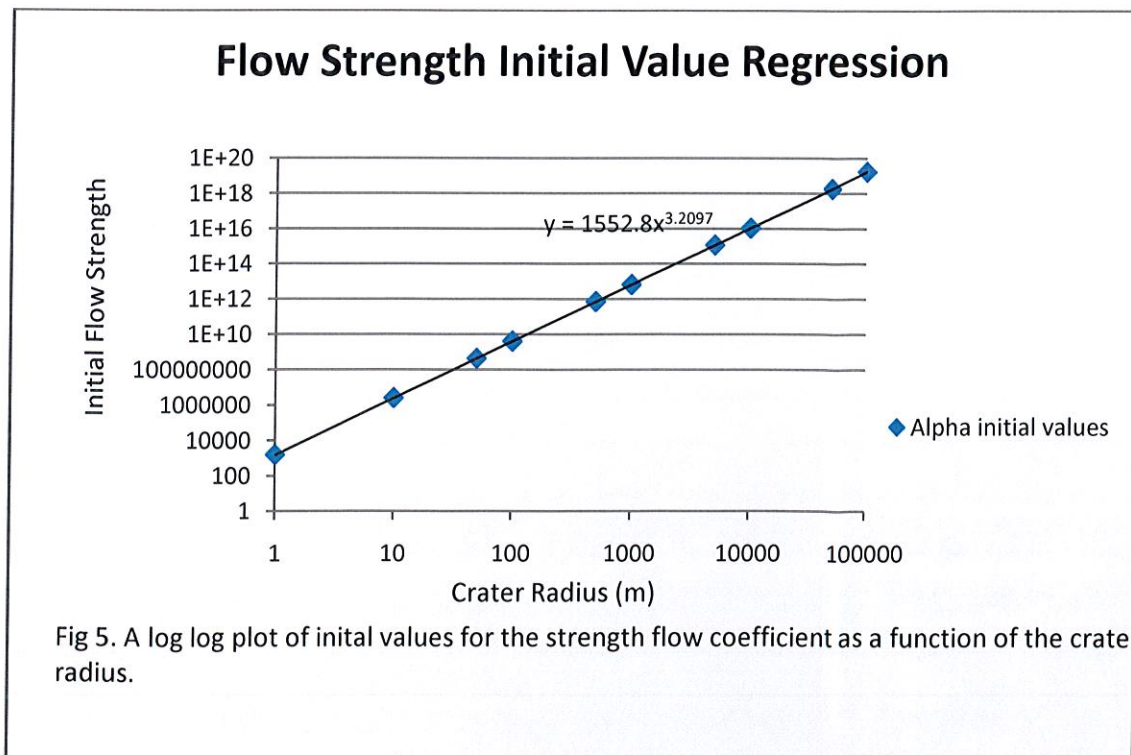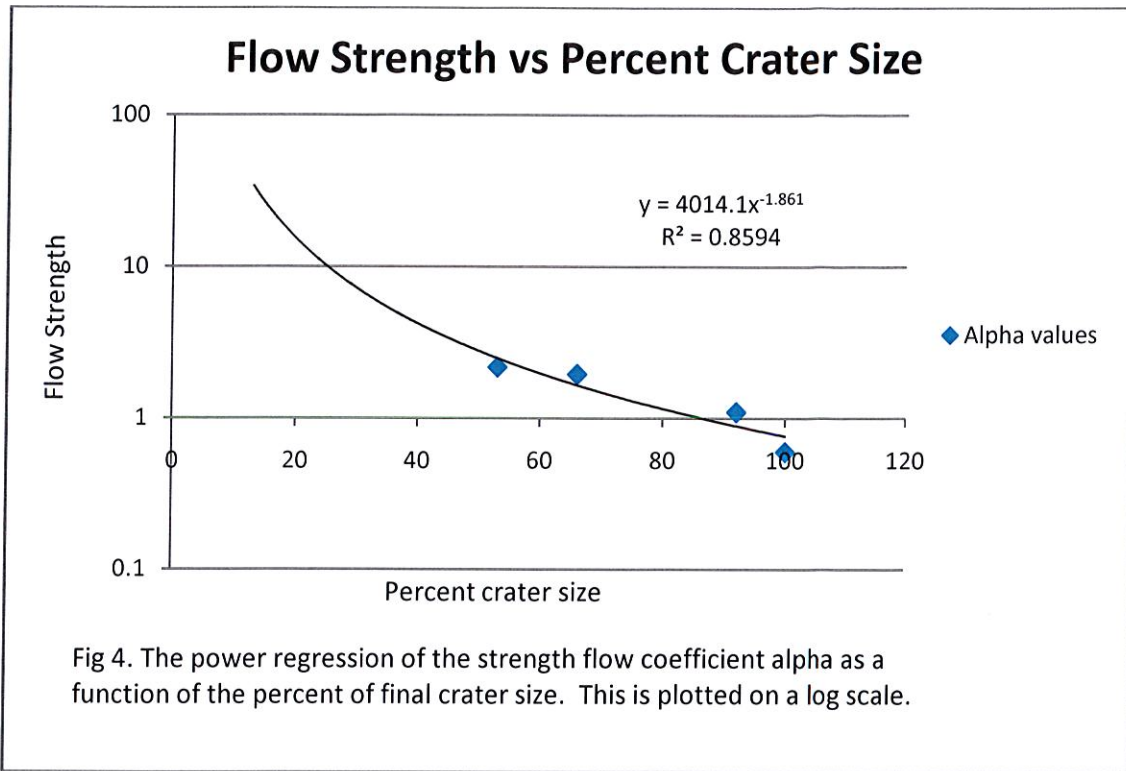
10) $4014.1 * Ra^{-1.861}$.

During the latter half of crater formation, the flow strength alpha declines by $\sim R^{-1.78}$. This is shown in

Fig 4, plotted with the y-axis on a log scale.

After this regression was applied to the data, it was discovered that the initial number in the function is dependent on the size of the crater. In other words, alpha gave realistic results for a calculated crater of one meter radius, but the function did not apply for larger or smaller craters. Another regression was developed so that the alpha function could be applied to any size crater. In doing this we recognized the initial number (4014.1) actually had to be dependent on crater size. We called this initial number α_0.

To find α_0 we recognized that in the last stages of ejecta flow, the final material trajectories should be nearly the same, leaving the distance for the final ejecta locations to be similar. This is a result of the overturned flap, as noted by Maxwell (1977) referring to the low energy trajectories of the final streamlines. Numbers were experimentally placed in the position of α_0 until the same value for the final two ejecta distances was attained. That number was plotted against the crater radius for which it was found. When several data points were established, a power regression was fit to the points plotted in a log-log scale. The result of the power regression is in Fig 5. In order to produce the required order of ejecta deposition, α_0 must increase as $\sim Ra^{3.2}$.

Flow Strength vs Percent Crater Size

$y = 4014.1x^{-1.861}$
$R^2 = 0.8594$

◆ Alpha values

Fig 4. The power regression of the strength flow coefficient alpha as a function of the percent of final crater size. This is plotted on a log scale.

Flow Strength Initial Value Regression

$y = 1552.8x^{3.2097}$

◆ Alpha initial values

Fig 5. A log log plot of inital values for the strength flow coefficient as a function of the crater radius.

Results

The data derived from this process has been formatted into a Microsoft Excel table that is dependent on the number entered in for apparent crater radius in meters. The table shows maximum depths for streamlines throughout crater growth as well as other geometric aspects of the crater morphology. This table has been included in an appendix for a crater of 10 km. Though streamline volumes were calculated for this project, they were not used in the final relations and so they have not been included in this table.

The maximum depths for the basalt were inferred assuming that any ejecta containing the low iron basement material could be detected in the Clementine imagery. The crater size was entered into the data table and the radius of basement material was related to the corresponding maximum streamline depth for that streamline. This only gives a maximum mare depth and is expected to be a high estimate because it is likely that basement material would not be detected at such a small percent of overall streamline volume.

Table 1. Locations and geometry of particular lunar craters and estimated basalt depths.

Crater	Lat (N)	Lon (W)	D (km)	radius b (km)	Thomson depth (km)	My estimate (km)
Carlini C.	33.7	24.1	10	n.a	>.84	>1.6
Herschel	34.5	31.2	13	n.a	>1.09	>2.1
Heis	32.4	31.9	14	n.a	>1.18	>2.2
Le Verrier	40.3	20.6	20	n.a	>1.55	>3.2
Pytheas	20.5	20.6	20	19.9	0.44	2.6-2.7
Helicon	40.4	23.1	24	n.a	>1.81	>3.9
Delisle	29.9	34.6	25	n.a	>1.9	>4
Euler	23.3	29.2	27	22.5	1.04	3.7-3.8
Lambert	25.8	21	30	n.a	>2.0	4.9
Timocharis	26.7	13.1	33	30.6	0.95	4.5
Autolycus	30.7	-1.5	39	35	1.17	5.3-5.5
Aristillus	33.9	-1.2	55	49.4	1.58	7.5-7.8

The crater data (location, Crater diameter (D) and radius of basement material (radius b) in the ejecta) were derived from Clementine images formatted by Thomson et al. in his current work. His inferred depths and my estimates for the maximum depths are shown. N.a in the radius column implies the lower layer wasn't reached.
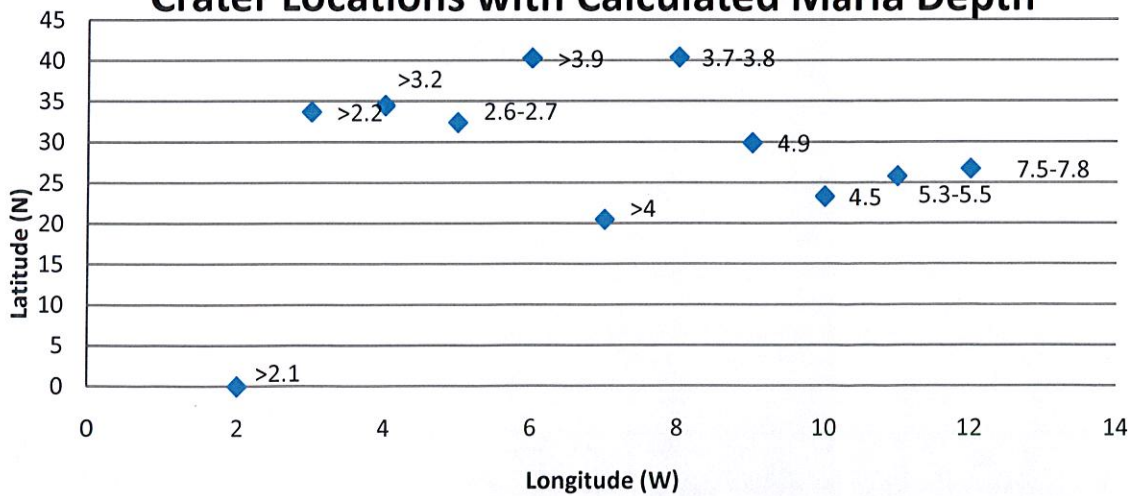
This table shows the locations of craters used in this study and my results for maximum basalt depth in those locations

Discussion

The data obtained for the geometric relations for a crater are reasonable and expected for the given conditions. The numbers are also roughly comparable to those found by Thomson et al. (2008). Our calculations show the basement ejecta to be deeper than Thomson's by a factor of about four. This is potentially the result of assuming that any basement material in the streamline will be apparent in the ejecta. It would be more realistic, however, to assume that the basement material will only be apparent as it approaches about 50 percent of the streamline volume. The data also shows a very clear trend toward a deeper calculated basement material for a larger crater. This flaw in the data is still unknown in origin but its consistency implies that it is derived from a single error.

There are a few issues of note with the assumptions made for this project. One of the major assumptions made was that craters shared the same morphology at nearly any size. It has however, been noted that the morphology for craters larger than 15 km may not in fact be accurately modeled by Maxwell's formulas (Head, 1975). This is also similar to the flawed assumption that all impacts are vertical when in fact they most likely are not (Shoemaker, 1962).

Initially it was assumed that the strength flow coefficient would be constant, however this resulted in inverted ejecta trajectories. A value for the strength flow ultimately based as a function of time is much more accurate; however the basis for our derivation of alpha may be flawed. The lab impacts used from Austin and Thomsen's research (1979, 1980) were based in plasticene clay, which has no particular shared similarity with lunar soil. In fact, a similar project done in gabbroic anorthosite material, which is similar to lunar material, yields very different results for the flow strength in terms of time (Austin 1981). We could not use this data, however, because of the lack of comparable

basement material as a percentage of the total streamline volume. The basement material should only be considered to be apparent when it approaches 50 percent of the total ejecta volume.

To develop the relations of basement material volume, one must first determine the volume of the entire streamline. This is done by Croft (1980) in his appendix.

$$11)\ Vsl = 2\pi \int_0^{Ro} \int_0^{90+\Delta} r^2\sin\theta\ dr\ d\theta + \frac{\pi}{3}d\ Ra^2$$

This is the volume from the streamline to the surface, and the volume of only the streamline can be deduced by subtracting the volume of the previous streamline from the next. To determine the total volume of the basement material within the streamline the equation for the streamline would be converted into two functions, one for each side of the maximum depth. Setting f(x) to be the function where x is greater than the maximum, and g(x) to be the function where x is less than the maximum, the volume could be determined as follows:

$$12)\ Vb = \pi \int_k (f(x)^2 - g(x)^2)dx$$

where k is the depth of the basement material. This volume would also have to be broken into streamlines and then percentages of the total streamlines derived.

To continue this project work would also be done to discover the cause for the trend in basalt depth correlated with crater size. This is an obvious flaw, but there is not time to ascertain the origins. It is suspected though, that it may actually be correlated with our alpha derivation. Along these lines, it would also be worthwhile to assess the accuracy of Thomson's assumption that material depth ratios are linearly correlated to ejecta material radius ratios.

Conclusions

Maxwell's model and derivations were used to relate original material depth to a final ejected distance from an impact crater. Data developed from these derivations was then applied to an estimation of maximum basalt thickness of lunar mare. These results were directly compared to similar estimates developed by Thomson (2008).

There were some interesting results from the process of deriving alpha that were mentioned in the discussion. These results include a correlation between the strength flow coefficient and the peak shock wave stress decay, which is expected but has not previously been noted in other work. The study of alpha also lead to some potential insight about the debate on final crater size scales from initial momentum and kinetic energy of the impactor.

It can be assumed that the process used to derive these basalt estimates is relatively accurate due to the similarity of the data to existing estimates. There is an obvious flaw in the data resulting in a deeper basalt depth estimate for a larger crater size that still needs to be addressed. Also it is important to establish that this method currently only derives the maximum possible depths of the basalt.

It would be worthwhile to recalculate these depths with a more accurate assessment based on a higher basement material content required for detection in the imagery. This would also bring the numbers into closer agreement with other conclusions on lunar basalt depth. These calculations would be made using volumes of the streamlines and volumes of material in the streamline below the mare.

References

Anderson J. L. B., Schultz P. H., Heineck J. T., 2003. The Evolution of Oblique Impact Flow Fields Using Maxwell's Z Model. Workshop on Impact Cratering, Geological Sciences, NASA Ames Research Center. 8031.pdf

Anderson J. L. B., Schultz P. H., Heineck J. T., 2003. Experimental ejection angles for oblique impacts: Implications for the subsurface flow-field. *Meteoritics and Planetary science*. 39.2, 303-320

Anderson J. L. B., Schultz P. H., 2006. Flow-field center migration during vertical and oblique impacts. *International Journal of Impact Engineering*. 33, p. 35-44.

Anderson J. L. B., Schultz P. H., Heineck J. T., 2001. Oblique impact ejecta flow fields: An application of Maxwell's Z model. Lunar and Planetary Science XXXII, Geological Sciences, NASA Ames Research Center. 1352.pdf

Austin M. G., Thomsen J. M., Ruhl S. F., Orphal D. L., Schultz P. H., 1980. Calculational Investigation of impact cratering dynamics: Material motions during the crater growth period, *proc. Lunar Planet. Sci. Conf. 11th*. p. 2325-2345.

Austin M.G., Thomsen J.M., Ruhl S.F., Orphal D.L., Borden W.F., Larson S.A., Schultz P.H., 1981. Z-Model analysis of impact cratering: An overview. *Multi-ring Basins, Proc. Lunar Planet Sci.*12A, 197-205.

Buchner E., Grasslin M., Maurer H., Ringwald H., Schottle U., Seyfried H., 2007 Simulation of
   trajectories and maximum reach of distal impact ejecta under terrestrial conditions:
   Consequences for the Ries crater, southern Germany. *Icarus*. (In Press)

Croft S. K., 1980. Cratering flow fields: Implications for the excavation and transient expansion stages
   of crater formation. Proceedings, 11t Lunar and Planetary Science Conference p. 2347-2378

Dahl, J. M. and P. H. Schultz (2001), Measurement of stress wave asymmetries in hypervelocity
   projectile impact experiments, International Journal of Impact Engineering, 26, 145-155

Dahl, Jason M; Schultz, Peter H (1999) In-target stress wave momentum content in oblique impacts,
   Abstracts of Papers Submitted to the Lunar and Planetary Science Conference, vol.30, abstr. no.
   1854

Gault D. E., Wedekind J. A., 1978. Experimental studies of oblique impact. Proceedings, 9th Lunar and
   Planetary Science Conference. p. 3843-3875

Head J. W., Settle M., and Stein R. S., 1975. Volume of material ejected from major lunar basins and
   implications for the depth of excavation of lunar samples. *Proc. Lunar Sci. Conf. 6th*, p. 2805-
   2829

Housen, K., 1984. Cratering Flow Fields: A General Form and the Z Model. *Shock Physics and Applied
   Mechanics*. MS 13-20, p. 377-378.

Housen, K R; Schmidt, R M; Holsapple, Keith A (1983) Crater ejecta scaling laws; fundamental forms

based on dimensional analysis, Journal of Geophysical Research, vol. 88, no. B3, pp.2485-

2499, 10 Mar 1983

Maxwell D. E., 1973. Cratering flow and crater prediction methods. Applied Mechanics Department,

Physics International Company. Technical memo TCAM 73-17

Maxwell D. E., 1977. Simple Z model of cratering, ejection and the overturned flap. *Impact and*

Explosion Cratering, edited by Roddy, D.J., Pepin, R.O., and Merrill, R. B., New York:

Pergamon Press p. 1003-1008

Melosh, H. J. (1989). *Impact Cratering: A Geologic Process*. 245 pp., Oxford University Press. New

York.

Shoemaker, E. M (1962), Interpretation of lunar craters. *Physics and astronomy of the Moon*, edited by

Kopal Z. New York: Academic Press. P. 283-351

Shoemaker, E. M. (1963), Impact Mechanics at Meteor Crater, Arizona, *The Moon Meterorites and*

Comets, edited by B. M. Middlehurst and G. P. Kuiper. Univ. of Chicago Press, Chicago. p.

301-336

Thomson B. J., Grosfils E. B., Bussy B. J., Spudis P. D., (Still in review). The thickness of mare basalts

in Imbrium Basin.

Thomsen J.M., Austin M.G., Ruhl S.F., 1979. Calculational investigation of impact cratering dynamics: Early time material motions. *Proc. Lunar Planet. Sci. Conf. 10th.* p. 2741-2756

Thomsen J. M., Austin M. G., Schultz P. H., 1980. The development of the ejecta plume in a laboratory-scale impact cratering event. Lunar and Planetary Institute, NASA Astrophysics Data System p. 1146-1148.

Appendix

Table 1: Data for a 10,000 meter crater

Key

Key	Value
Z	2.712
G (m/s^2)	1.62
Radius (m)	10000
EDOZ (m)	1380
α0	1E+16

%final Ra	Ra	Rs	Δ (deg)	Ro	Ym	α	Ur	Uθ	Ux	Uy	φ (de)	X(G)
0.2	2000	2429.897	34.606	1674.930	1706.660	3.983E+13	26624.587	36010.112	1463.115	44759.983	88.128	80752916.829
0.25	2500	2855.591	28.899	2101.125	1789.780	2.63E+13	11348.549	13651.259	3338.236	17435.671	79.161	71771151.569
0.3	3000	3302.181	24.702	2554.637	1878.228	1.873E+13	5452.175	6041.644	2428.412	7767.270	72.638	23260873.459
0.35	3500	3762.233	21.519	3025.483	1970.056	1.406E+13	2873.918	2997.895	1573.963	3843.100	67.728	7462066.207
0.4	4000	4231.359	19.034	3507.513	2064.066	1.097E+13	1630.229	1623.735	1011.534	2066.631	63.920	2581641.372
0.45	4500	4706.846	17.049	3996.895	2159.510	8.807E+12	981.106	942.224	661.740	1188.468	60.891	974237.355
0.5	5000	5186.945	15.430	4491.190	2255.911	7.239E+12	619.796	577.964	443.689	722.032	58.429	400015.761
0.55	5500	5670.485	14.085	4988.816	2352.963	6.062E+12	407.678	371.049	305.120	459.108	56.392	178229.104
0.6	6000	6156.655	12.953	5488.725	2450.459	5.156E+12	277.446	247.437	214.924	303.330	54.681	86385.923
0.65	6500	6644.878	11.986	5990.208	2548.263	4.442E+12	194.389	170.394	154.763	207.050	53.223	46011.320
0.7	7000	7134.732	11.152	6492.779	2646.279	3.87E+12	139.657	120.613	113.691	145.348	51.968	27375.637
0.75	7500	7625.903	10.426	6996.100	2744.441	3.404E+12	102.552	87.432	85.037	104.546	50.875	18462.159
0.8	8000	8118.152	9.787	7499.931	2842.702	3.019E+12	76.765	64.710	64.648	76.817	49.917	14123.393
0.85	8500	8611.295	9.222	8004.101	2941.030	2.696E+12	58.447	48.778	49.874	57.513	49.069	12036.923
0.9	9000	9105.185	8.717	8508.488	3039.400	2.424E+12	45.178	37.369	38.992	43.785	48.314	11105.140
0.95	9500	9599.708	8.265	9013.003	3137.795	2.192E+12	35.398	29.047	30.855	33.834	47.637	10787.234
1	10000	10094.771	7.857	9517.581	3236.202	1.993E+12	28.076	22.874	24.686	26.498	47.027	10806.551

This table shows the data for a 10 km crater, the assumptions for variables are noted previously.